A radiometric calibration for the Clementine HIRES camera

Mark S. Robinson

Center for Planetary Sciences, Northwestern University, Evanston, Illinois, USA

Erick Malaret

Applied Coherent Technology Corporation, Herndon, Virginia, USA

Travis White

Lawrence Livermore National Laboratory, Livermore, California, USA

[1]   We have successfully characterized the Clementine HIRES multispectral sensor entirely from inflight measurements. Relative calibration is obtained through dark subtraction (additive) and sensor spatial nonuniformity (multiplicative) on a pixel-by-pixel basis. Relative residuals from frame-to-frame are typically less than 1%. Absolute coefficients are obtained through comparisons with calibrated Clementine UVVIS images acquired nearly simultaneously with HIRES sequences. Residuals between the coregistered UVVIS and HIRES calibrated images are typically 5% but may be as high as 20%. The residual is found most likely to be the result of increased scattered light in the UVVIS relative to the HIRES. Application of the calibration allows for seamless mosaicking of monochromatic and color sequences aiding in interpretation of surface features of the Moon at the scale of about 25 m/pixel. The calibrated HIRES color sequences represent the highest resolution spectral image data of the Moon.   *INDEX TERMS:* 5494 Planetology: Solid Surface Planets: Instruments and techniques; 6250 Planetology: Solar System Objects: Moon (1221); 6297 Planetology: Solar System Objects: Instruments and techniques; 5462 Planetology: Solid Surface Planets: Polar regions; 5464 Planetology: Solid Surface Planets: Remote sensing; *KEYWORDS:* Clementine mission, spacecraft, HIRES camera, Moon, calibrated, scattered light

1. Introduction

[2]   The Clementine spacecraft imaged the Moon over 1.8 million times during the spring of 1994 with four dedicated science cameras: ultraviolet-visible (UVVIS), near-infrared (NIR), high resolution (HIRES), and the long-wave infrared (LWIR). The UVVIS and NIR cameras allow for the determination of visible and near-infrared (415–2780 nm) global color at a spatial resolution of 100–360 m/pixel over 11 bandpasses [*Nozette and Garrett*, 1994; *Nozette et al.*, 1994; *McEwen and Robinson*, 1997]. The LWIR acquired pole-to-pole image strips for each orbit at a spatial resolution of ∼65 m/pixel. The HIRES camera acquired image sequences to construct single band mosaics (750-nm) of the polar regions (∼30–60 m/pixel) and limited acquisitions of four-color strips over targets of scientific interest. The color strips were generally acquired with phase angles less than 50° to emphasize the spectral content of the image data rather than the black and white morphologic information acquired with the polar mosaic sequences. The purpose of this paper is to document a radiometric calibration of the HIRES camera providing an estimate of both absolute and relative accuracy.
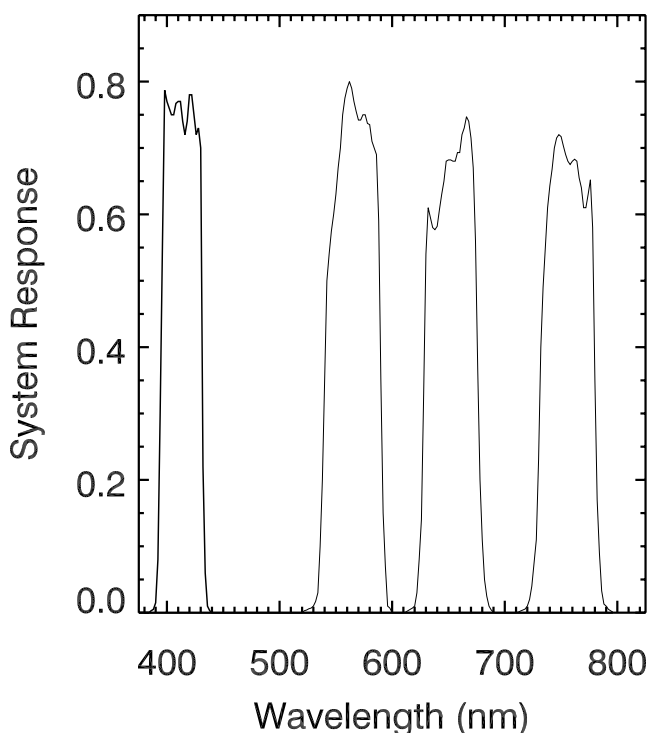
[3]   The HIRES camera (Figure 1) consisted of a light-weight telescope, a six-position filter wheel, and an image intensifier coupled with a frame transfer CCD detector (total instrument weight 1120 g). Shuttering was accomplished by cycling the image intensifier. The instrument had a narrow field view (0.4° by 0.3°), allowing for an effective resolution of about 20–60 m/pixel during the Clementine mapping orbits. The filter wheel had four narrow color bands (415-nm, 560-nm, 650-nm, and 750-nm; Figure 2), a clear filter for navigation, and an opaque shield for the intensifier used during LIDAR operations (the Clementine laser-ranger (LIDAR) shared the HIRES optics) [*Nozette et al.*, 1994].

[4]   The HIRES image data contain three distinctive sensor generated features: hexagonal chicken-wire pattern, hot spot (Figure 3) (both features are a result of the image intensifier), and in certain cases a hysteresis associated with the MicroChannel Plate (MCP) gain setting [*White and Wilson*, 1994]. The first two problems have been addressed by synthesizing flat-fields for each spectral filter from image data acquired while in lunar orbit. The third feature, hysteresis, is more problematic. After a change in gain state from filter-to-filter the HIRES imaging system sometimes
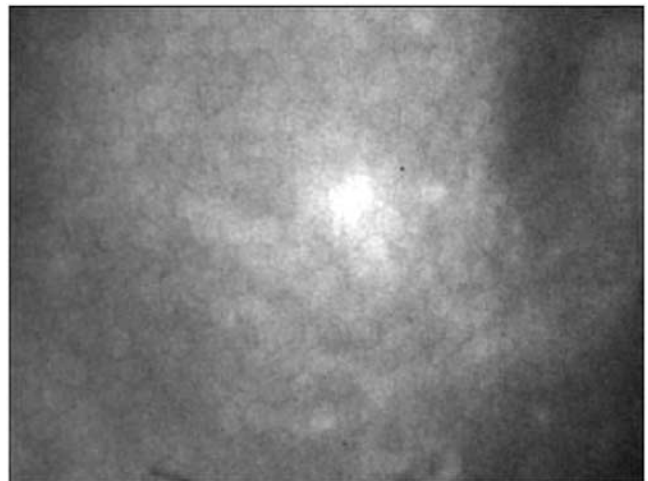
Figure 1. Photograph of Clementine HIRES camera (courtesy Lawrence Livermore National Laboratory).

Figure 3. Low-contrast raw HIRES frame of the surface of the Moon showing chicken wire mesh pattern and hot spot introduced by the image intensifier into all the Clementine HIRES frames. Peak to trough in each cell of the mesh pattern is typically 10% of the average scene radiance, while the hotspot is greater than 50% of the average scene radiance. These artifacts greatly hinder use of the raw frames for any scientific interpretation (frame lhd0532e.222, latitude −49.9°, longitude 213.6°).

contained a partial "memory" of the previous gain state, which effectively resulted in an unknown multiplicative factor being applied to the image immediately following a gain change, if the second image was shuttered within a short time of the first. The gain memory (hysteresis) affects only the first image after a gain change. The exact cause of the hysteresis is not known [*White and Wilson*, 1994]. Unfortunately, the gain hysteresis occurs for a portion of the color strips (for some or all the filters) when the sensitivity/radiance differences for each bandpass were

accounted for with changes in MCP gain rather than integration time. When images were acquired in rapid sequence cycling through the filter wheel, hysteresis resulted in brightness differences of greater than 10% from frame-to-frame for some orbits, thus necessitating an empirical correction derived from areas of overlap between affected frames.

[5] Many of the HIRES images were intentionally set to a constant value at the time of acquisition as part of the LIDAR ranging experiment [*Nozette et al.*, 1994]. These constant value images are stored on the Clementine Planetary Data System archive CDROMs because their associated ancillary data contain an important record of camera conditions potentially useful for calibration purposes. These images do not represent lost data. Details of the mission and data acquisition strategies appear elsewhere [*Nozette et al.*, 1994; *Sorensen*, 1995; *McEwen and Robinson*, 1997].

[6] As the starting point for the in-flight calibration presented here, a camera model based on prelaunch calibration data) was utilized. We note that none of the prelaunch calibration data have been made available and the entire calibration presented in this paper was derived from data acquired while in lunar orbit. The camera model allows for the conversion from instrument counts (or DN values) measured, with a given set of camera parameters, to a calibrated estimate of apparent radiance for any given pixel. The vast majority of useful HIRES images were acquired with an exposure time of 1.07 ms and a gain state of 4. Most variation in camera sensitivity was accomplished with changes in the MCP gain state (image intensifier) and/or offset. The procedures used to obtain all the calibration data are discussed in the

Figure 2. HIRES instrument total system spectral response for the four mapping filters (a) 415-nm, (b) 560-nm, (c) 650-nm, and (d) 750-nm.

Table 1. Summary of Key Image Parameters for the HIRES Color Sequences of the Moon Utilized in This Study (Latitudes Between 85°S to 85°N and Slant Distances Less Than 10, 000 km)[a]

Parameter	Orbits 1−166	Orbits 167−350
Gain	a: 4	a: 1, 4
	b: 4	b: 4
	c: 4	c: 4
	d: 4	d: 4
Integration time, ms	a: 1.07	a: 0.15, 1.07
	b: 1.07	b: 1.07
	c: 1.07	c: 1.07
	d: 0.01, 1.07, 10.00, 10.67	d: 1.07, 10.00
Offset id	a: 5 b: 5 c: 5 d: 3, 4, 5	a: 4, 5 b: 5 c: 5 d: 5
	b: 5	b: 5
	c: 5	c: 5
	d: 3, 4, 5	d: 5
MCP gain	a: 143, 144, 146, 148	a: 148, 151, 153, 156, 159, 162, 165, 166, 171
	b: 129, 130, 132, 134	b: 117, 119, 122, 123, 125, 128, 131, 135, 139, 141
	c: 134, 135, 137, 139	c: 137, 140, 142, 145, 148, 151, 155, 160
	d: 5−166	d: 142−166
FPA temperature	a: 269.03−279.00	a: 269.03−279.85
	b: 269.38−273.42	b: 269.12−272.00
	c: 269.38−273.42	c: 269.20−279.00
	d: 250.00−276.87	d: 250.00−279.30
Emission angle	a: 0.41−2.42	a: 0.38−30.00
	b: 0.42−2.44	b: 0.38−29.98
	c: 0.42−2.46	c: 0.22−29.88
	d: 0.01−29.95	d: 0.14−29.99
Incidence angle	a: 12.91−41.03	a: 17.37−90.00
	b: 12.93−41.05	b: 17.36−86.35
	c: 12.94−41.07	c: 17.34−86.47
	d: 0.12−90.00	d: 2.34−90.00
Solar Phase angle	a: 12.70−39.05	a: 17.36−86.48
	b: 12.72−39.06	b: 17.35−86.39
	c: 12.73−39.08	c: 17.33−89.97
	d: 0.16−90.00	d: 2.1−89.07
Compression ratio	a: 11.58−72.09	a: 5.72−72.09
	b: 8.42−14.50	b: 6.02−71.86
	c: 10.60−17.58	c: 6.11−71.58
	d: 5.97−72.24	d: 5.23−72.28
Number frames	a: 150	a: 3460
	b: 158	b: 2923
	c: 158	c: 2343
	d: 190176	d: 56864

[a]Notations a, b, c, and d refer to HIRES bandpasses 415-nm, 560-nm, 650-nm, and 750-nm, respectively.

following sections together with estimates of the associated errors.

2. In-Flight Calibration Data From Vega Images

[7] Important to this calibration are observations of Vega obtained during almost every orbit of the lunar mapping phase of the mission by the HIRES camera. HIRES images of Vega were identified by a search of the mission ephemeris keying on right ascension and declination from which 3338 images were identified. Of these images only those that passed a signal-to-noise threshold test were kept as part of the analysis,

$$\text{if max value} > \text{mean value} + (\text{stdev} \times 4.75) \qquad (1)$$

where max value is the pixel with the largest DN from a 19×19 pixel brightness centroid, stdev is the standard deviation of the 19×19 pixel centroid, and the 4.75 factor was empirically determined from an iterative inspection of the data. This selection process left 1840 images for the statistical analysis. For a given angular pointing error the

absolute error in pixels increases linearly with instantaneous field-of-view. Thus of the cameras carried by Clementine the HIRES camera was most sensitive to pointing jitter. The camera pointing uncertainty for the HIRES resulted in a random spread of the location of Vega in the field-of-view from image-to-image over a range of 200 lines and samples (average sample. line position (245, 140) with standard deviations (37, 31)) ensures that no spatial vagary of the system will unduly influence the derived values.

3. Background Characterization

[8] All 1840 valid images taken of Vega were utilized in the HIRES background estimation. After locating Vega in the image an iterative procedure was used to determine optimal sizes of both a large box ($M \times M$) and a smaller box ($N \times N$) centered on Vega. The nonintersecting region between the small and large box was used to determine the local background. After processing all the Vega images and iterating M and N we found $M = 19$ and $N = 13$ to give the optimal values for background and Vega contribution for offset state code 0. The center (smaller box, known as the BlobSum) contains the radiance contribution from Vega
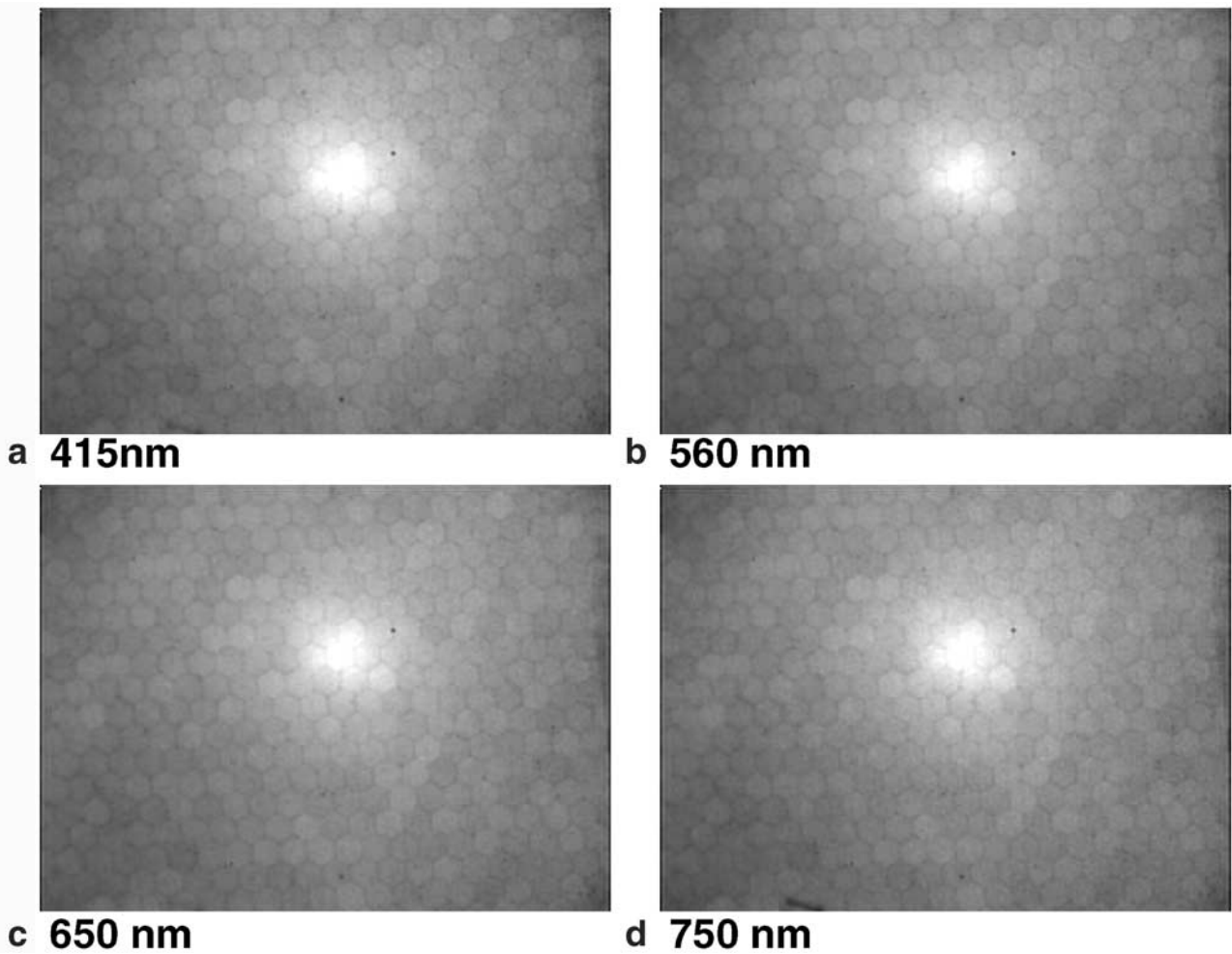
Figure 4.   Flat field files synthesized for each of 4-filter bandpasses from image data of the Moon for the Clementine HIRES camera. (a) 415-nm, (b) 560-nm, (c) 650-nm, (d) 750-nm.

(including energy spread from the star). The nonintersecting region of the larger box (LargeSum 19 × 19) and the BlobSum was used to determine the background.

$$\text{Background} = \frac{\text{LargeSum} - \text{BlobSum}}{M^2 - N^2} \qquad (2)$$

[9] All of the Vega observations were acquired with an offset state of zero. Thus we were forced to use images acquired of nonilluminated portions of the Moon taken before and after crossing the southern and northern terminators (respectively) for offset states of 4 and 5. From the Vega and near-terminator observations we fit a line to determine background as function of offset id ($y = -8.1811x + 49.261$, $r^2 = 0.9996$) for all offset states used during lunar mapping (offset ids 3, 4, 5; Table 1).

4. Nonuniformity Estimation

[10] As discussed above, the HIRES image data contain a distinctive hexagon chicken-wire pattern and a hot spot (both a result of the image intensifier). These features were modeled by synthesizing a flat field for each filter from images acquired of the Moon (Figure 4). From the complete set of lunar HIRES images a subset was selected for inclusion in the flat field derivation on the following criteria: mean value >50 after background subtraction, no more than 9 pixels could have values greater than 250 (8-bit system), offset id value less than or equal to 5, center latitude between 75°S and 75°N, emission angle less than 10°, and phase angle greater than 10°. This sorting procedure located 1,426 450-nm images, 530 560-nm images, 1039 650-nm images, and 500 750-nm images. Preprocessing for these images included background subtraction and normalization to each image's own mean value. For a given filter, all preprocessed images were stacked in a cube and the median value at each pixel was found and transferred to the nonuniformity matrix. The assumption we made was that with enough images acquired over random areas of the Moon (excluding shadows), each pixel on average sees average Moon. A similar procedure was used to derive the nonuniformity estimates for the Clementine UVVIS camera [*Malaret et al.*, 1999].

5. Point Spread Function Estimation

[11] The image intensifier introduces a blurring effect or degradation of the point spread function (PSF). We used the
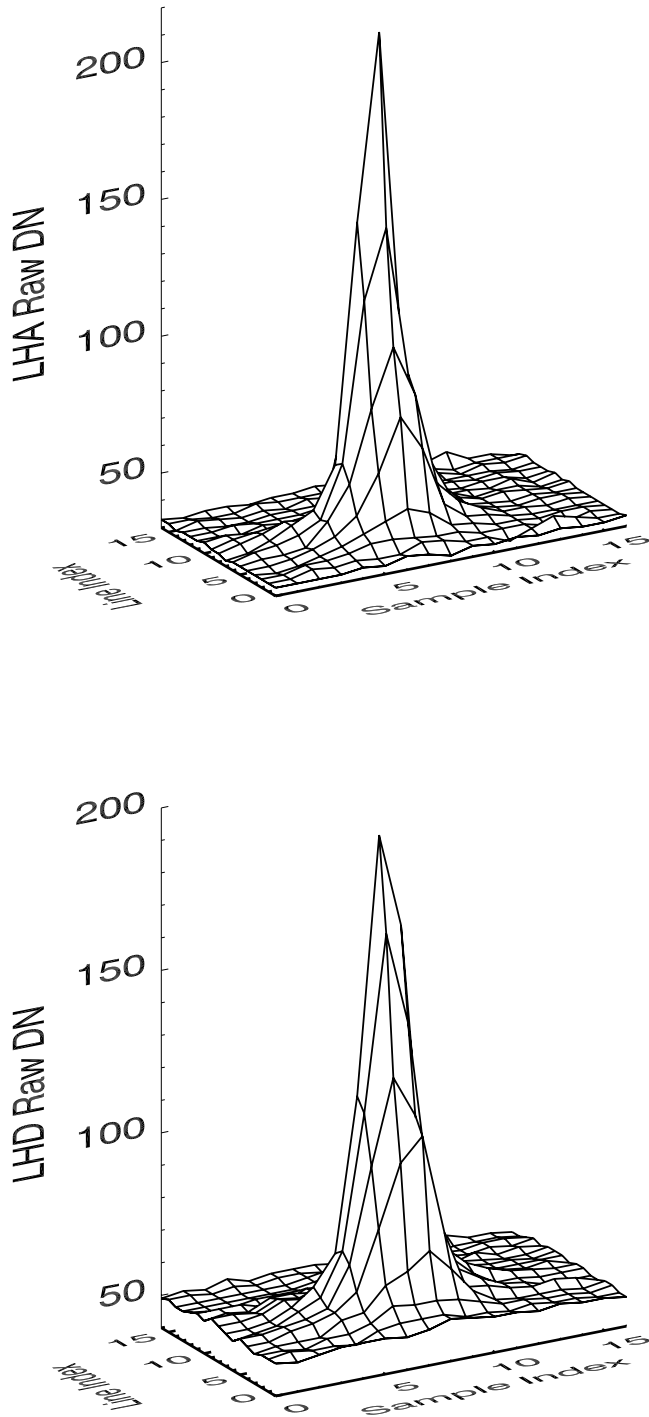
Figure 5. Clementine HIRES camera Vega observations (raw data) from Orbit 250 showing the system's PSF (top) frame lha5780y.250, (bottom) frame lhd5783y.250. In an ideal system the star would appear as a single pixel spike above a uniform background.

Vega observations to estimate the HIRES system's PSF by examining the spread of energy from the peak pixel within the BlobSum (center of 13 × 13 box, see above). The full width half maximum (FWHM) for each color filter in both the line and sample directions ranged between two and three pixels (Figure 5), resulting in a degradation of the instru-

ment's effective spatial resolution by about a factor of three. Because of this degradation we commonly resample the HIRES data for mosaicking purposes by a resolution factor of three using an averaging scheme. This subsampling effectively raises signal-to-noise ratio by a factor of about 3 (square root of 9), an important benefit because much of the HIRES image data has raw DNs typically between 50–100 out of a possible raw range of 0–255. Additionally the data generally suffered lossy compression onboard the spacecraft (~10×) [*Nozette et al.*, 1994], which serves to lower the effective SNR of an image.

6. Scattered Light

[12] Determining an absolute calibration coefficient for the HIRES image data has proven problematic. We initially had planned to use the Vega observations. However, the Vega observations were taken at combinations of gain state and MCP gain state that do not match with the HIRES observations of the Moon. Thus we used areas of overlap in coregistered partially calibrated HIRES and fully calibrated UVVIS images to derive absolute coefficients for the HIRES data. The HIRES partial calibration consisted of background subtraction and flat fielding. One way to derive the absolute coefficient (per filter) is by fitting a line to the coregistered UVVIS and HIRES mosaics (Figure 6), at the same filter settings. Ideally the best fit line would go through the (0, 0) intercept (using identical filters), and the slope would be used as the absolute coefficient to convert the HIRES data to absolute units. However, we found that the best fit line does not pass though the (0, 0) intercept (Figure 6). In fact, there is a large negative offset (−10.3, where the mean of the calibrated HIRES mosaic is 50.1). On the positive side, the UVVIS/HIRES comparison does show that the HIRES response is linear. Initially, this large negative offset raised concerns about the validity of our HIRES offset correction. A logical explanation was that an overcorrection was applied to the HIRES offset (or the UVVIS was being undercorrected). As a check on the validity of the HIRES offset correction, shadows in several hundred dark corrected HIRES frames, acquired near the North Pole, were examined for evidence of an offset problem (see Appendix A for a summary of results). Typically the shadow values, after offset correction, are about 1–2 DN (where brightly illuminated areas typically have raw DNs of ~80); these shadow values are thought to be the result of reflected light from nearby topographic facets and/or scattered light and are not consistent with a gross error in our offset correction. A similar check was performed on UVVIS data (E. Eliason, USGS, personal communication, 1999), and no UVVIS offset residual problem was detected.

[13] Other possible explanations for the offset discrepancy (Figure 6) are contrast degradations due to the gross spatial resolution differences between the two sensors (12 m/pixel for HIRES, 170 m/pixel UVVIS) and/or differential scattered light. To compare the UVVIS and HIRES data on a pixel-by-pixel basis, we resampled each dataset to the same spatial resolution (200 m/pixel). The resampling of the HIRES data was accomplished by an averaging scheme that resulted in a large gain in the SNR and the effective
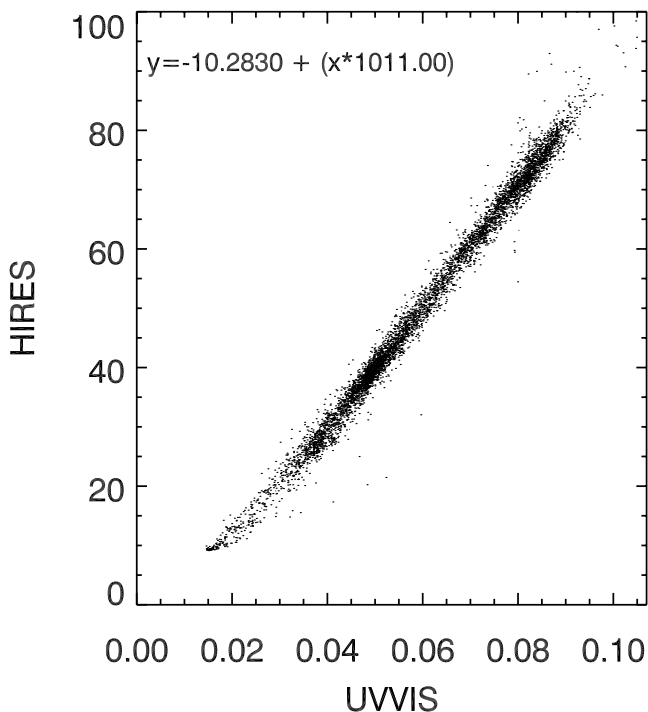
Figure 6. Scatter plot of HIRES versus UVVIS coregistered mosaics described in text (orbit 082). In an ideal case a best fit line to these data should pass through (0, 0) and the inverse of the slope would serve as an absolute coefficient for the HIRES data (correcting for integration time, gain states, and absolute sensitivity). From these data it is apparent that there is a large negative y-intercept (see text for discussion).

simulation of a nearly perfect PSF, while the UVVIS data were sampled close to their original resolution. Thus the HIRES mosaic appears relatively sharp at high frequency boundaries despite the matching resolutions. We then blurred the HIRES mosaic to match the apparent sharpness of the UVVIS data (match the effective PSF) by iterating on low pass filters (LPF) of various window sizes applied to the 200-m/pixel HIRES mosaic. We found, through visual inspection that at a scale of 200 m/pixel a 3 × 3 LPF applied to the HIRES data resulted in the best match between the HIRES and UVVIS mosaics. This filtering slightly improved the y-intercept value from −10.3 to −8.6. (a 5 × 5 LPF resulted in −6.0 y-intercept, but the HIRES data were noticeably blurred compared to the UVVIS). Thus we conclude that vagaries of exactly matching the PSF and SNR of the UVVIS with the grossly oversampled HIRES data cannot account for the large negative offset residual (Figure 7).

[14] We believe that differences in scattered light effects between the UVVIS and HIRES instruments are the main cause of the offset residual. If the HIRES instrument had relatively less scattered light component and the UVVIS had relatively larger scattered light component one would expect the large negative intercept (Figure 6). Light scattered from outside the field-of-view of the CCD can be grossly thought of as an additive factor to the whole image (Figure 7c). In reality this additive component has a

low-frequency shape related to variations in the brightness of the scene (outside the CCD field-of-view surrounding the image). This type of additive component would result in a translation of the scatter plot to the right, causing a negative y-intercept (assuming UVVIS or x-axis had the worst scattered light). Light scattered from within the field-of-view results in a reduction of contrast: bright materials have a net loss of energy, while dark materials have a net gain of energy (especially important around high contrast boundaries), which results in a counterclockwise rotation of the plotted data about the mean value of the x-axis (UVVIS data; Figures 6, 7). One can imagine the extreme case where the UVVIS camera is completely defocused; every pixel in the image is the same. The HIRES/UVVIS plot would in this case consist of a vertical line centered on the mean value of the UVVIS frame. To further investigate this problem, we examined three types of images: (1) images with no illumination from outside the CCD field-of-view, (2) images containing mostly deep space with a small amount of bright limb showing, and (3) relatively large shadows as far from the pole as possible (thus maximizing the brightness of target outside the CCD field-of-view).

[15] During the systematic mapping of the Moon the UVVIS camera imaged the Earth many times after passing the northern terminator. These data are suitable for quantifying light scattered only within the field-of-view of the CCD (no target outside the CCD's field-of-view). Ideally, images of a point source (stars) would be used to determine the PSF, however the sensitivity of the UVVIS was such that star images have poor signal-to-noise [*Malaret et al.*, 1999]. A profile traversing the Earth shows that energy spread from the disc drops rapidly, and within 30 pixels plateaus off at a level less than 2% of the maximum value within the profile for the UVVIS (Figures 8, 9). In contrast, a highly oblique UVVIS image of the lunar limb containing mostly space (Figures 10, 11) shows that the energy spread from the Moon is above 8% of the maximum lunar surface value (within the profile) 30 pixels from the Moon: the profile plateaus at about 4% of the maximum DN over 200 pixels from the Moon. In this test a large bright target (the Moon) lies outside of the field-of-view of the CCD (but within the field-of-view of the optics). The data presented in Figures 8–11 indicate that light scattered from outside the field-of-view of the CCD dominates the total scattered light within a UVVIS image. We note that the image of the Earth (Figures 8 and 9) has a phase angle of 5° and the limb image (Figures 10–11) has a phase angle of 89°.

[16] Unfortunately, there are no resolved targets smaller than the HIRES field-of-view, so a test exactly analogous to the UVVIS data of the Earth is not possible. However, the Vega derived HIRES PSF estimates indicate that the total area in pixels over which incoming energy is spread is comparable to the UVVIS instrument (compare Figure 5 and see *Malaret et al.* [1999]) for point targets with no target outside the CCD field-of-view. Recall that the FWHM for the HIRES is ∼2X coarser than that of the UVVIS (mostly due to energy spreading by the light intensifier) but here we are comparing the total spread of energy. A profile across a HIRES image of the Earth (recall that portions of the Earth lie outside the CCD's field-of-
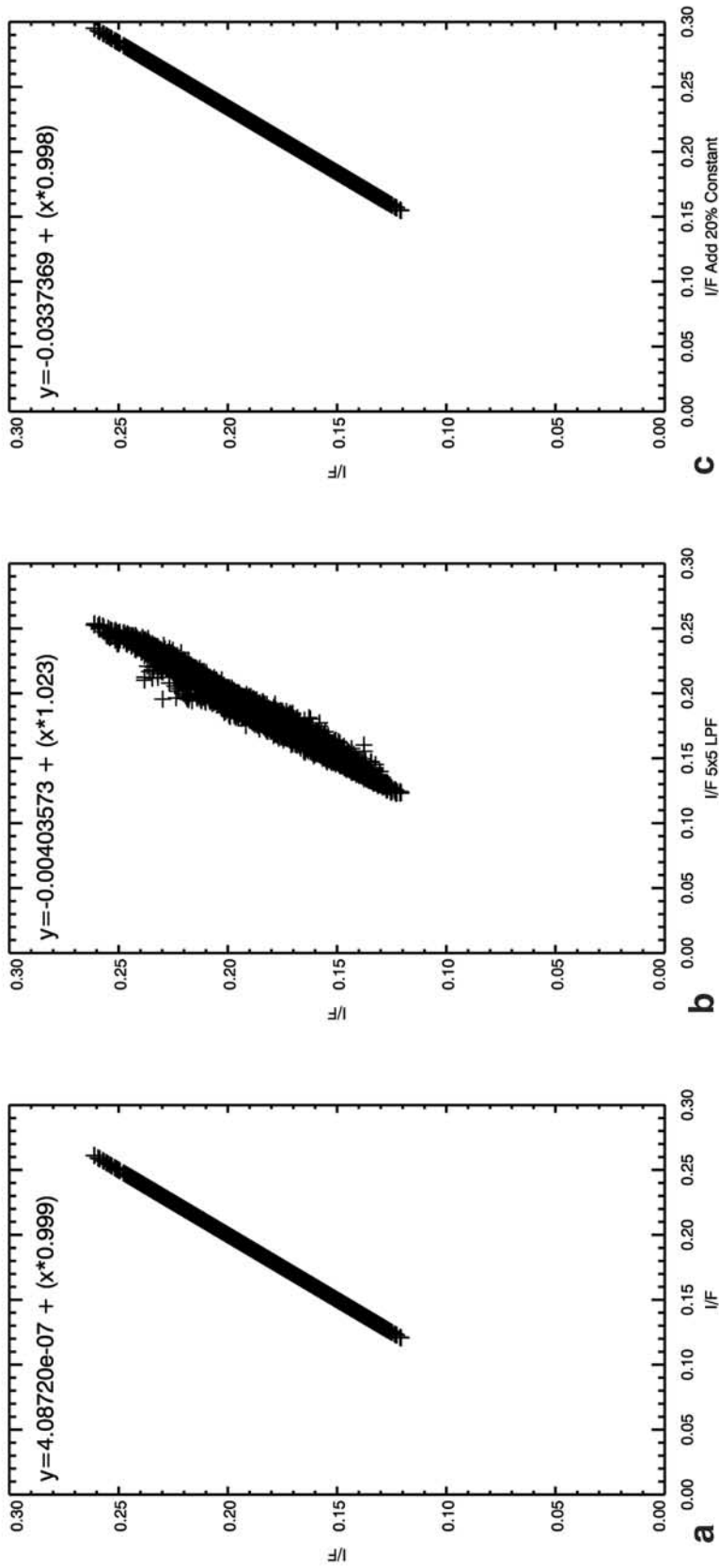
Figure 7. (a) Scatter plot of perfectly correlated data (lub5052n.086 plotted both x and y axes) showing (0, 0) intercept and slope of 1. (b) Simulated degradation of PSF, same data as in Figure 7a with a 5 × 5 low pass filter applied to the x-axis data only. Note that the slope is steeper with a negative offset. This example is relevant to the comparison of UVVIS and HIRES due to the gross difference in resolution (effective PSF). (c) Same data as in Figure 7a with an additive constant (0.034, 20% of the mean value of the image), applied to the x-axis data only. The resulting negative y-intercept is ~16% of the mean of the additive-enhanced image.
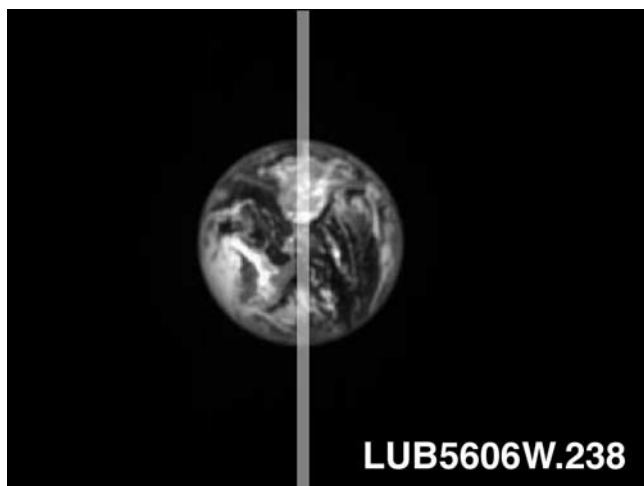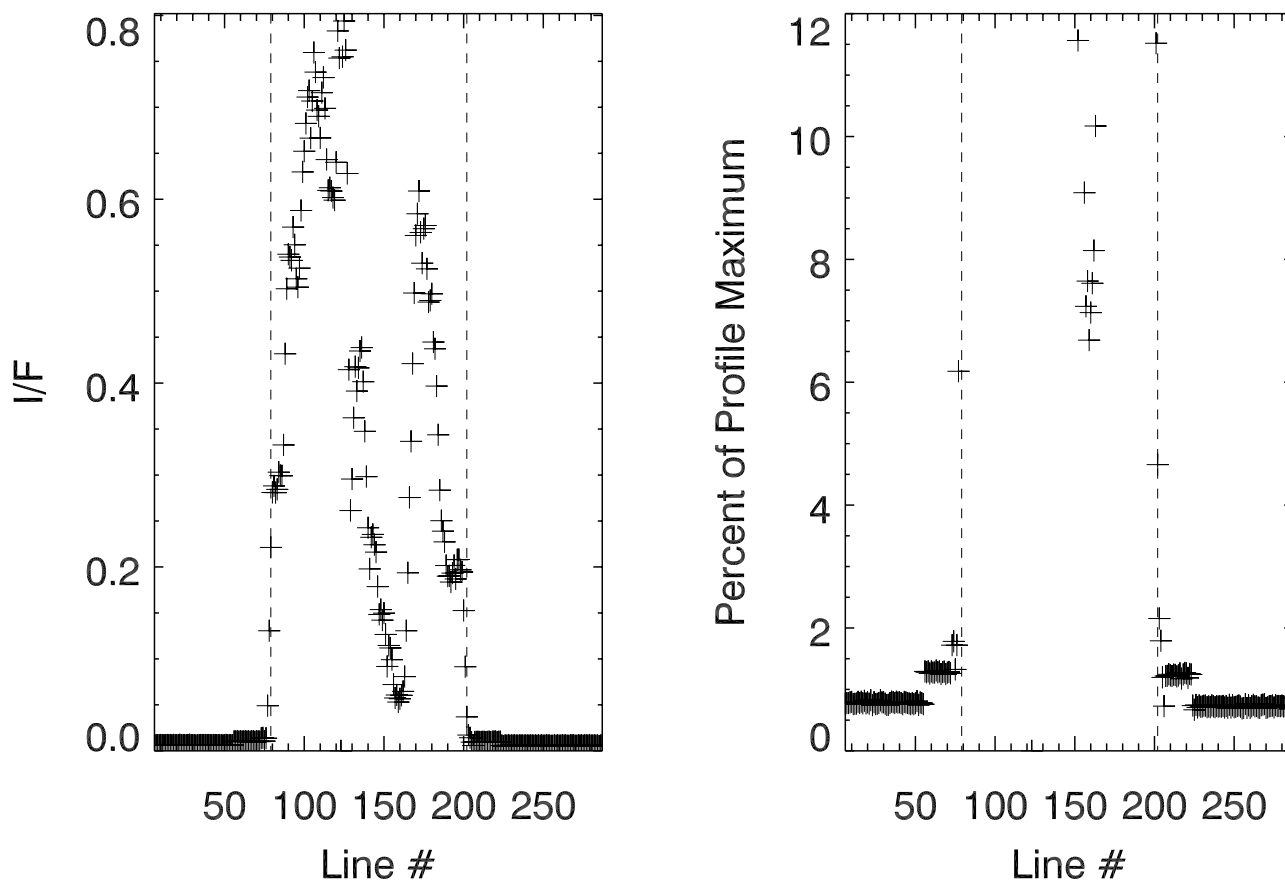
Figure 8. Clementine UVVIS Earth full disk image, median of 7 values centered on column 177 (shown by stripe) plotted in Figure 9 (frame lub5606w.238).

view but within the optics field-of-view) shows the residual DNs in space drop off to a plateau of ~2% of the brightest value within 30 pixels of the Earth (Figures 12–13). Compare this with the UVVIS lunar limb plot (Figures 10, 11) where the analogous plateau occurs about 200 pixels

from the limb and the plateau level is 4% of the maximum value.

[17] A final comparison of UVVIS and HIRES scattered light was made utilizing images acquired during the same sequence of a resolved shadow in the Schrodinger basin (Figures 14–19). The shadow indicated in Figure 14 was specifically picked because it is formed from a massif and thus does not have a bright Sun-facing wall (as would be found in an impact crater) reflecting light into the shadow. This strategy minimizes the mount of ''allowed'' scattered light and more accurately portrays light scattered by the instrument. In the UVVIS data the shadow is approximately 50 pixels wide; the DNs plateau in the shadow at a value of >20% the area value (AV) that corresponds to relatively horizontal ground close to the shadow (Figures 14, 15). Figure 16 shows the same shadow as imaged by the HIRES camera shuttered within seconds of the UVVIS frame (Figure 14); thus the lighting conditions were essentially identical. The HIRES values drop off to a plateau of 10–15% of the AV in the first frame (Figure 17) which contains some illuminated lunar surface and then drops to a steady plateau of about 5% of the area value in the next HIRES frame (Figure 18) which images only shadowed area.

[18] From these data it follows that the magnitude and spreading of the HIRES instrument's out-of-field scattered light component is significantly less than that of the UVVIS instrument. Our comparisons of calibrated brightness


Figure 9. Clementine UVVIS Earth full disk profiles plotted as I/F (left), and normalized to maximum value in profile (right); dashed lines indicate boundaries between Earth and space (see Figure 8).
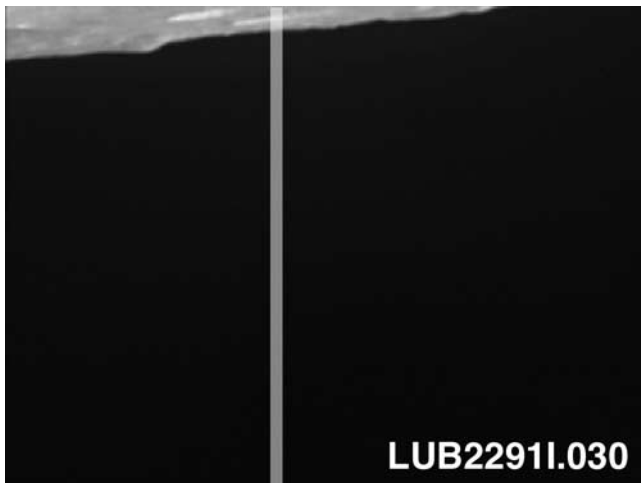
Figure 10. Clementine UVVIS image showing lunar limb. Stripe indicates location of data; median of seven pixels centered on column 162, plotted in Figure 11 (frame lub2291i.030, incidence angle ∼27°, center of limb at 6°S latitude, 15° longitude).

between the HIRES and UVVIS, especially in areas of contrast boundaries, thus should exhibit a residual in the sense seen in Figure 6, a negative offset when plotting HIRES versus UVVIS values. We cannot say with certainty
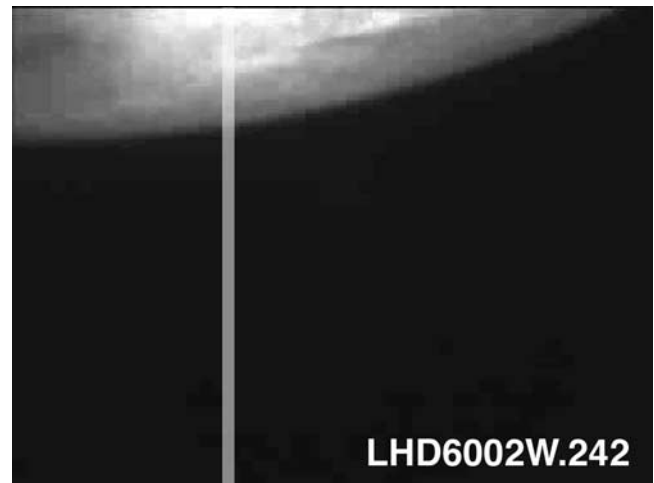
Figure 12. Clementine HIRES frame (lhd6002w.242) showing Earth's limb and deep space. Stripe shows location (column 129) of data plotted in Figure 13.

that the residual is mostly due to this effect, but our observations are consistent with this hypothesis.

7. Absolute Coefficient and Scattered Light

[19] We examined four HIRES color strips acquired in the South Pole-Aitken region of the lunar farside and 63
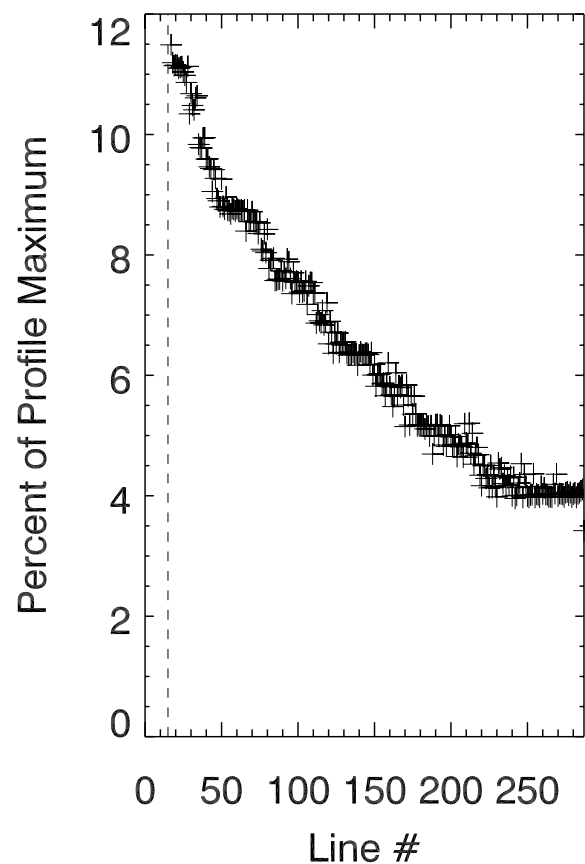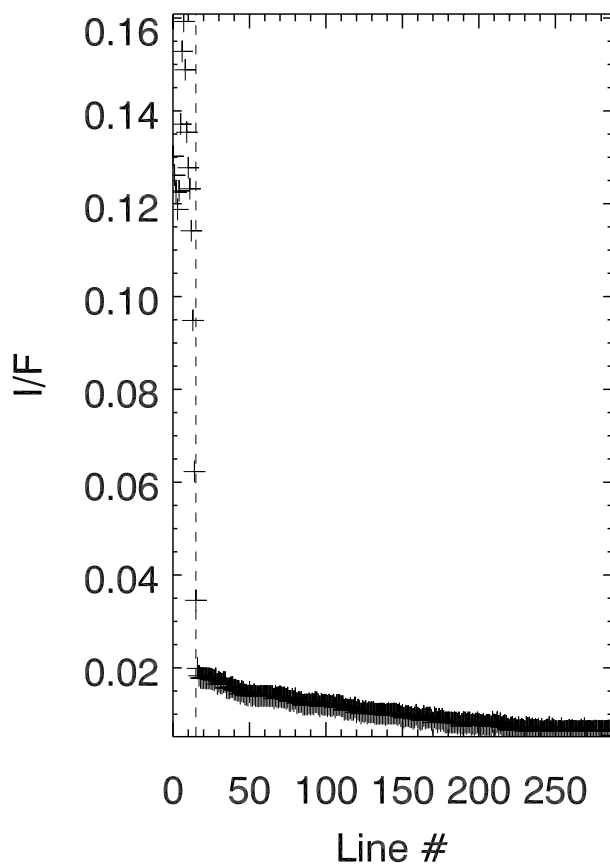
Figure 11. Clementine UVVIS Lunar limb data. Each point median of seven pixels in sample direction; dashed line indicates limb and space boundary. Data plotted as I/F (left) and normalized to maximum value in profile (right).
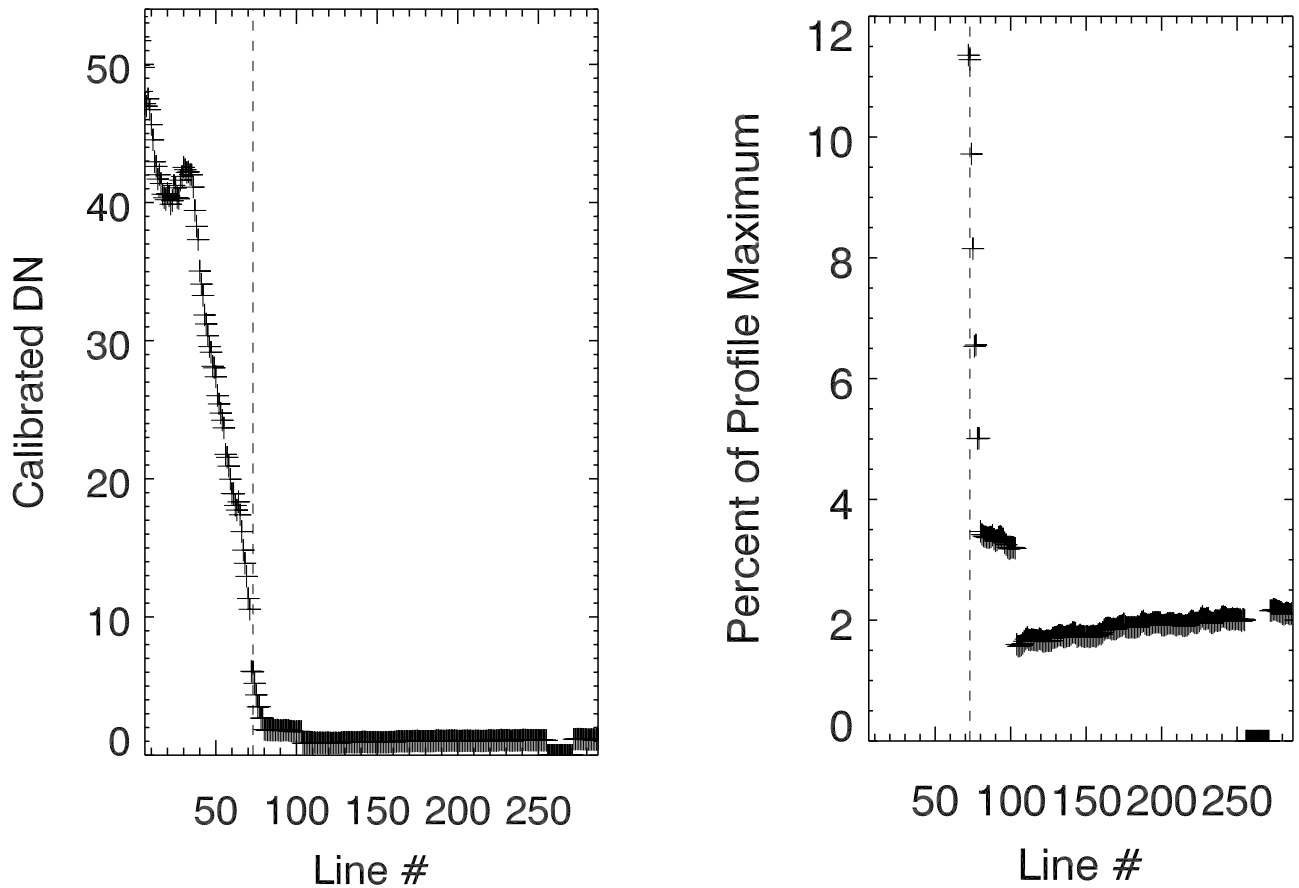
Figure 13. Profile from image shown in Figure 12. Earth's limb ends at line 73 (indicated by dashed line). Each point along profile is the median value of seven pixels in the sample direction. Data plotted as I/F (left), and normalized to maximum value in profile (right).

monochromatic orbit strips covering the North Pole region to derive absolute coefficients for the HIRES 415-nm and 750-nm filters (Tables 2–4). Initially, we had hoped that by fitting UVVIS I/F [*Minnaert*, 1960] mosaics (I_{UVVIS}) and HIRES partially calibrated (P_{HIRES}) mosaics per filter

$$I_{UVVIS} = P_{HIRES} \times m + c \qquad (3)$$

we would find a near zero offset and the multiplier would simply serve as the absolute coefficient. However, as described above, the constant term is nonnegligible (Table 2–4). Not only is the term nonnegligible, but both the constant and multiplier vary by more than 10% upon inspection of various 200 pixel regions within a given mosaic (Tables 3–4). This observation begs the question, what does this tell us about the data? We have attempted to show that scattered light from outside the CCD FOV is greater in the UVVIS camera than in the HIRES camera. Taking the derived fits and applying them to the HIRES data, would result in absolute calibration of HIRES data in units of I/F, also including the UVVIS scattered light component (c in equation (3)). However, applying an additive factor to the P_{HIRES} mosaic results in a nonlinearity being introduced: darker areas would receive a larger percentage change than brighter areas. The
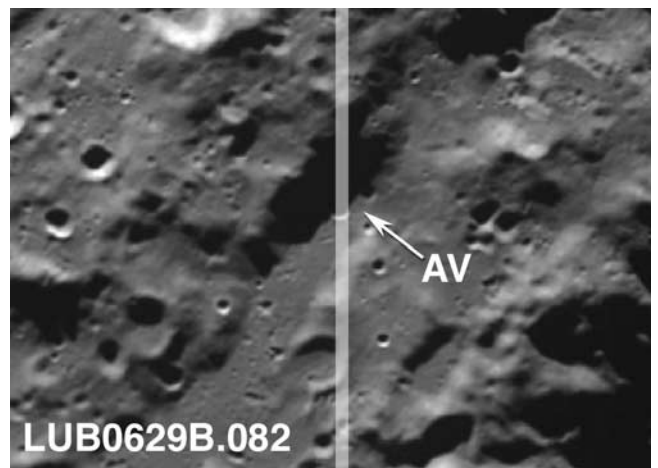
Figure 14. Clementine UVVIS frame showing location used to compare resolved shadow values in both UVVIS and HIRES data. Shadow is crossed by profile indicator just to the northwest of the normalization area indicated with AV (frame lub0629b.082, center latitude 79.4°S, longitude 128.17°, 171 m/pixel, 63 km wide, north to the top).
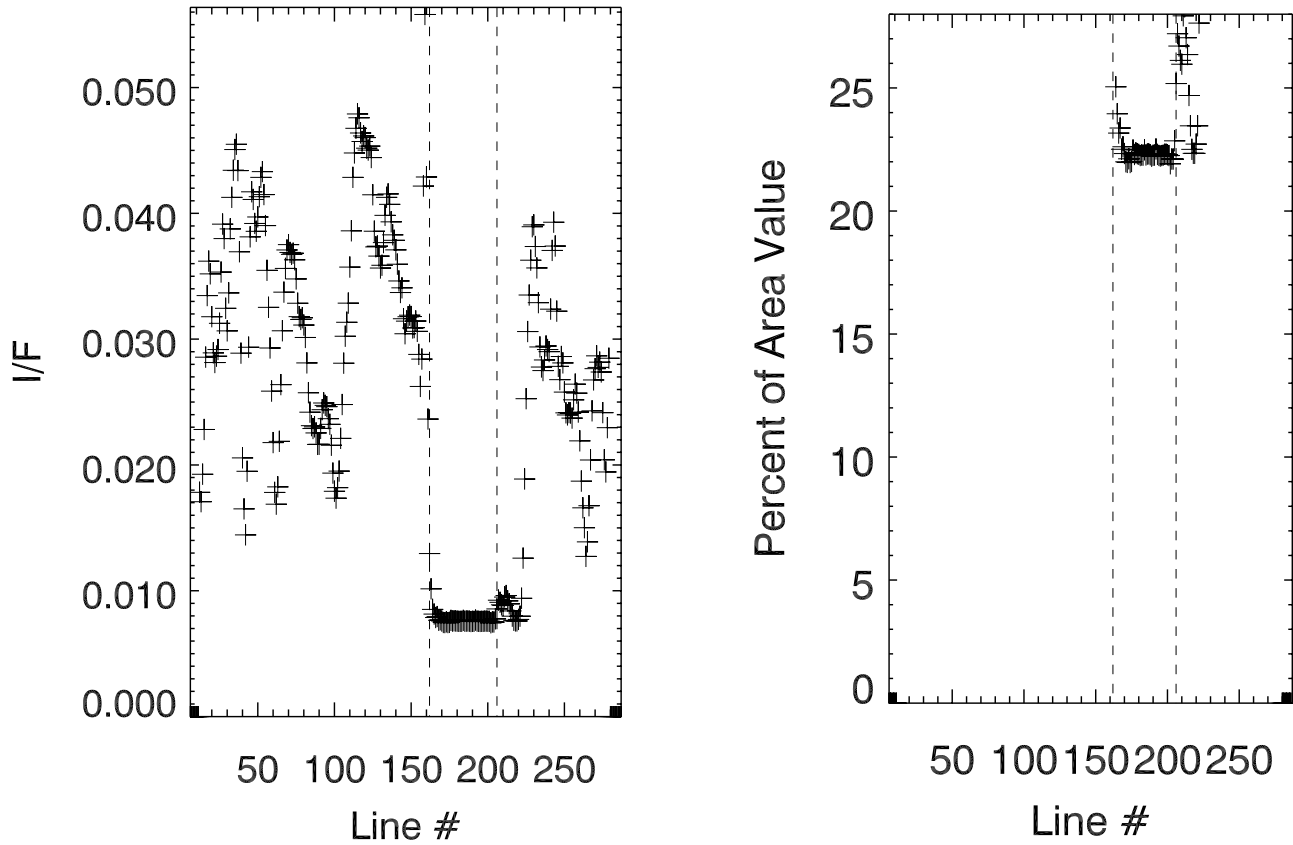
Figure 15. Plot of data seen in profile indicated in Figure 14, lub0629b.082, column 185. Average of 7 pixels (3 pixels to each side of column 185); dashed lines indicate edges of shadow. On the right the data have been normalized (and converted to percent) to the area value (AV in Figure 14) illuminated by the Sun just outside the shadow. Note that the residual in the shadow is >20% the value of the surrounding terrain.

constant term (c) can be used as a coarse estimate of the scattered light component in the UVVIS instrument (assuming negligible scattered light in the HIRES). Taking the c values at face value, the UVVIS has a scattered light component of 27% for the 415-nm (lua) for both orbits 214 and 220, and 17% and 16% in the 750-nm (lub) for orbits 214 and 220, respectively. A full analysis of scattered light in the UVVIS instrument is beyond the scope of this paper, however we conclude that it is significantly greater than 10% in both the 415-nm and 750-nm filters.

[20] Unfortunately, no systematic four-color strips were acquired of the lunar nearside that have adequate SNR and pointing stability. If such data existed they might be compared to Earth-based telescopic measurements to avoid the conflicting scattered light issues explained above. An alternate approach to deriving the absolute coefficient to the partially calibrated HIRES frames is to simply ratio the regions of overlap between the I_{UVVIS} mosaic and the P_{HIRES} mosaic and calculate the average value of the resultant ratio image.

$$K_\lambda = \frac{I_{UVVIS}}{P_{HIRES}} \qquad (4)$$

This value (K_λ) is the absolute coefficient to apply to the partially calibrated HIRES frames within a given set of

camera settings (for 415-nm and 750-nm) to convert to units of I/F [*Minnaert*, 1960]. The ratio values (K_λ) derived from orbits 214 and 220 are stable to ~1% (Tables 3, 4). This strategy avoids the introduction of a nonlinearity but simply ignores any scattered light problem. The absolute coefficient can be found for images with any MCP gain setting by using a first order fit to the K values presented here, assuming that gain state and offset id are set to 4 and 5, respectively (which includes the vast majority of HIRES frames of the Moon). The precision of this ratio derived absolute coefficient is about 5%, found from inspection of the standard deviation of the ratio images (Tables 2, 3). A summary of the ratio derived absolute coefficients is presented in Tables 5 and 6.

[21] For the two spectrally unique HIRES bandpasses (560-nm and 650-nm) we simply assumed a straight-line continuum between the fully calibrated HIRES 415-nm and 750-nm mosaics and estimated linear coefficient values for the remaining two HIRES filters.

$$K_{560, mcp} = \frac{((145/335) \times (I_{750} - I_{415})) + I_{415}}{P_{560, mcp}} \qquad (5)$$

$$K_{650, mcp} = \frac{((235/335) \times (I_{750} - I_{415})) + I_{415}}{P_{650, mcp}} \qquad (6)$$
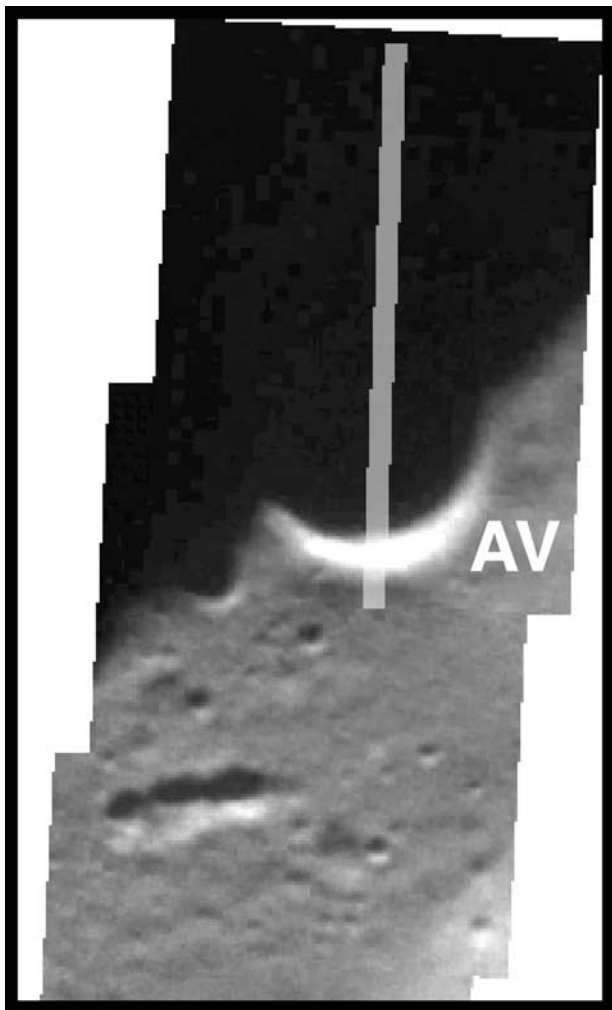
Figure 16. Clementine HIRES shadow image mosaic of images lhd0624b.082, lhd0631b.082, lhd0637b.082, 25 m/pixel, strip ∼4.5 km wide. Area labeled AV shows location of area value used to normalize HIRES data (Figures 17, 18). AV corresponds to the same geographic area used to normalize UVVIS data shown in Figures 14 and 15.

The constants 145, 235, and 335 are the respective $\Delta\lambda$. With the other unknowns in the derivation of the absolute coefficients for the 415-nm and 750-nm bandpasses and the generally monotonic spectral properties of the lunar soils between 415-nm and 750-nm, this is a reasonable first order assumption (e.g., see Figure 1 in *Charette et al.* [1974] for mare units observed telescopically and Figure 1 in *Charette et al.* [1976] for highlands soils observed in the laboratory). There are cases, especially regional dark mantle deposits, where this assumption may not strictly hold true. However, with the limited data presented here and the lack of a definitive absolute calibration of the lunar surface this assumption is generally acceptable. The consequence of this assumption may be a slight underestimate of the actual absolute radiance of a few percent for the 560-nm and 650-nm data. Later improvements in absolute sensitivities for the HIRES data could easily be derived by an individual analyst based on newly acquired data.

[22] The calibration presented here can be implemented with the following equation.

$$I_{HIRES(\lambda,o,g,mcp,i,j)} = \frac{R_{HIRES(i,j)} - B_o}{N_{\lambda,i,j}} \times K_{\lambda,mcp} \qquad (7)$$

I_{HIRES} is the final calibrated HIRES value in units of I/F [*Minnaert*, 1960]. R_{HIRES} represents the raw HIRES image data, B is the background per offset state (o), N is the nonuniformity matrix per wavelength (λ), and K is the absolute coefficient per wavelength (λ) and MCP gain state. Terms with the i,j subscript indicate pixel-by-pixel corrections, while those without are global constants.

8. Conclusion

[23] Solely from in-flight data we have obtained a relative calibration to 1% or better in four spectral filters for the Clementine HIRES camera. After applying this calibration and geometrically controlling to the Clementine UVVIS basemap, HIRES strip mosaics can be assembled into useful scientific products representing the highest resolution digital images of the Moon, both monochrome and color (Figures 19, 20). The HIRES coverage of the polar regions are particularly useful for mapping morphology and regions of excessive shadow or illumination at the highest ever resolution (25 m/pixel) [*Shoemaker et al.*, 1994; *Bussey et al.*, 1999]. Absolute calibration derived by comparisons with overlapping areas of UVVIS data results in residuals as high as 20%. It is our interpretation that much of this residual is due to differences in scattered light between the two instruments. Our preliminary investigation of scattered light characteristics in the UVVIS instrument (in support of the HIRES calibration) shows that a detailed investigation of the UVVIS scattered light problem would be beneficial to scientific interpretation of high-frequency albedo and color boundaries. The lack of preflight calibration data greatly hampers the interpretation of both the UVVIS and HIRES scattered light characteristics and thus derivation of a UVVIS based absolute coefficient(s) for the HIRES bandpasses. However, the residuals in the absolute calibration do not negate the usefulness of the data for most scientific purposes.

[24] The present calibration allows unimpeded use of color ratios to investigate relative color properties such as cataloging immature crater populations, downslope movement of regolith and gross compositional differences. A full characterization of scattered light in both instruments will allow an improvement in absolute brightness, key to quantifying compositional differences. Pioneering work deriving compositional abundances (FeO and TiO_2) for lunar soils utilizing the Clementine 415-nm, 750-nm, and 950-nm UVVIS data by *Lucey et al.* [1995, 1998] underscores the potential value of these calibrated HIRES image data. A cursory examination of the HIRES color mosaics (Figure 20) in both normalized I/F and ratio values (i.e., 950-nm/750-nm and 415-nm/750-nm) indicates that relative color trends should allow for similar compositional analyses at greatly increased resolution. We note that at the spatial scale of the resampled HIRES color strips (25−50 m/pixel) brightness variations are dominated by local topography and not by compositional or maturity differences as is true for the
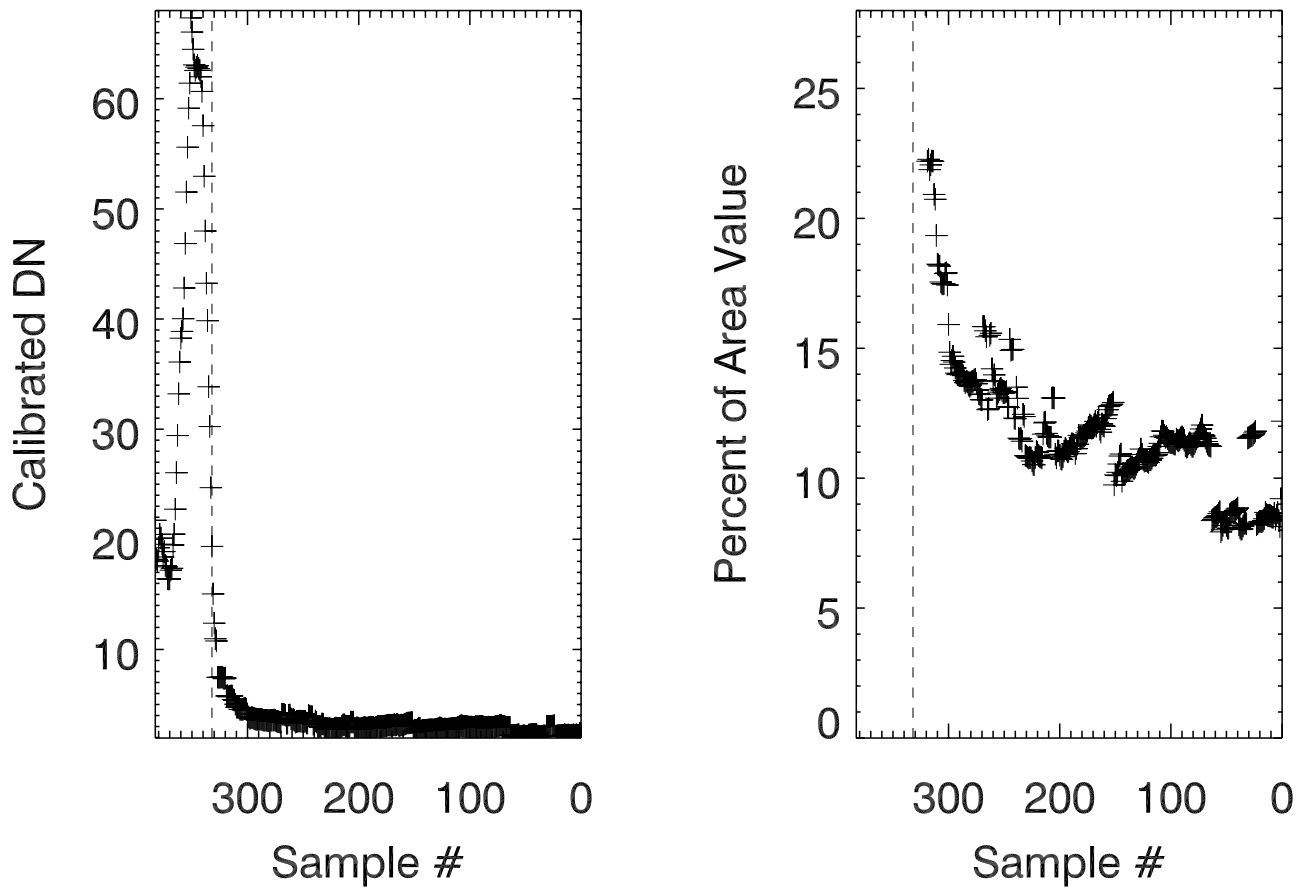
Figure 17. Clementine HIRES shadow image plot, data from column 133 of image lhd0637b.082 (top frame of mosaic shown in Figure 16); right side normalized to area value (marked AV in Figure 16), see also Figures 14 and 15. Data points represent median value of seven samples centered on profile shown in Figure 16; dashed line indicates edge of shadow.
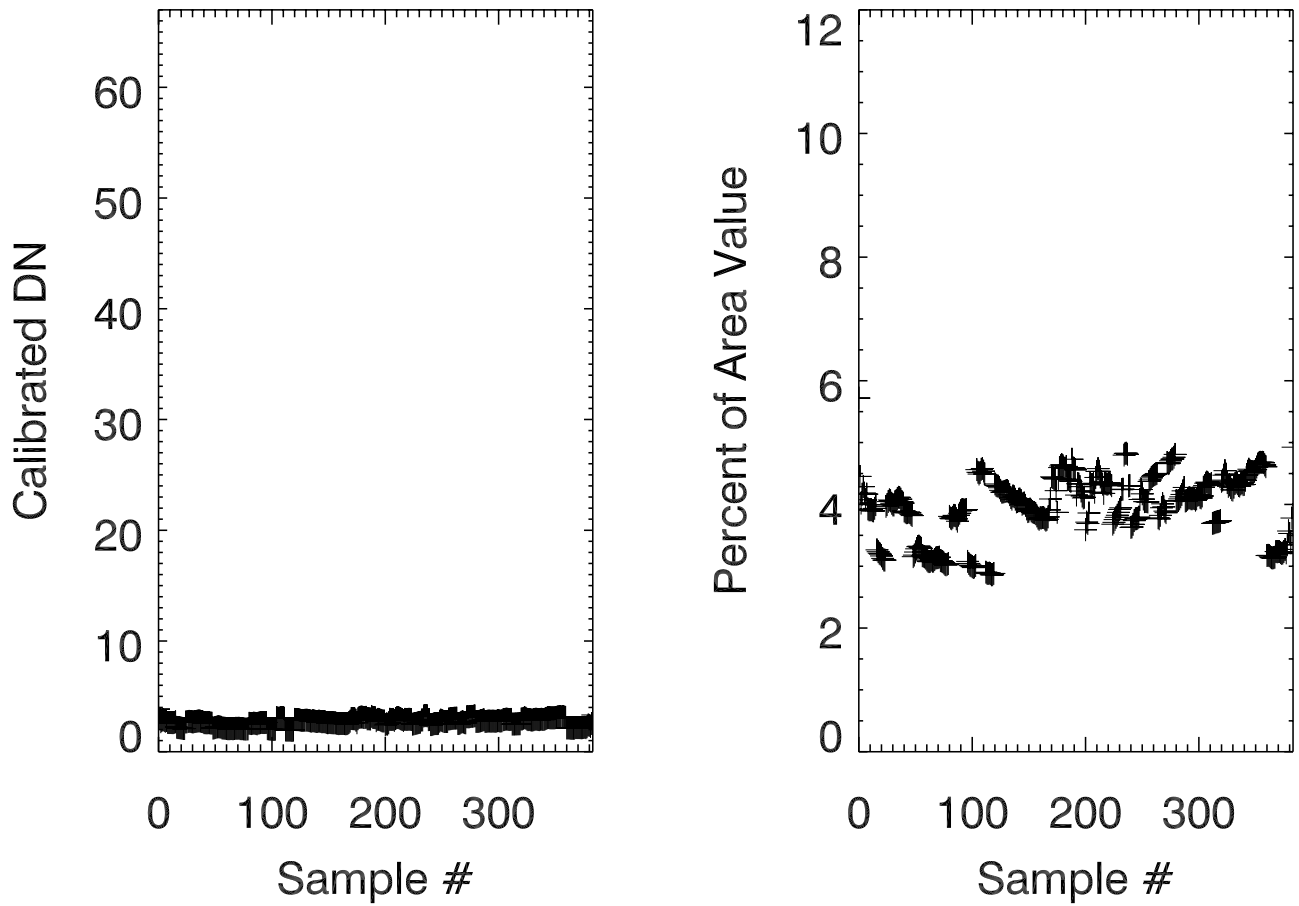
Figure 18.   Profile crossing shadow in HIRES frame lhd0638b.082 (not shown) corresponding to same shadow examined in UVVIS data (Figures 14 and 15). These data are a continuation of the mosaic shown in Figure 16 and the plot shown in Figure 17. Frame lhd0638b.082 contains no illuminated surface; the area it covers is completely shadowed. Data are normalized to area value (AV) indicated in Figure 16.
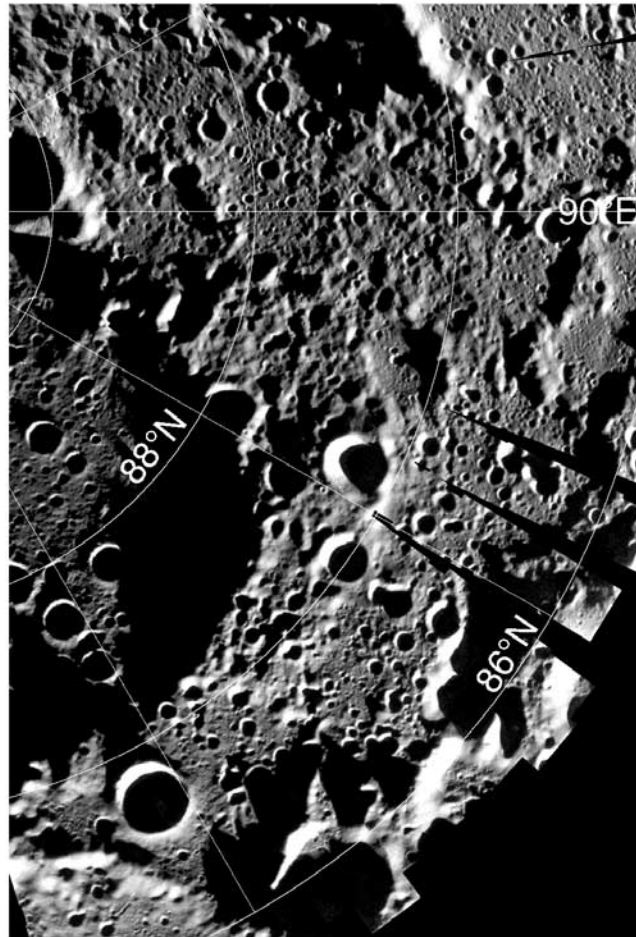
Figure 19. Portion of a North Pole Mosaic formed from 63 orbit strips (Orbits 46–161; 1009 frames) from month 1 of the Clementine mission. No attempt was made at seam removal; relative brightness residuals between frames is <1% after application of calibration presented in this paper.

Table 2. Fits Between HIRES and UVVIS Mosaics Per Camera Settings[a]

	MCP	Average	Ratio	Constant (c)	Mult (m)	R	Hysteresis
Orbit 214							
UVVIS 415	-	0.051	-	-	-	-	-
UVVIS 750	-	0.096	-	-	-	-	-
HIRES 415	159	57.5	0.00088696	0.013219	0.000654	0.94	No
HIRES 560	128	118.4	-	-	-		Yes
HIRES 650	148	51.1	-	-	-		Yes
HIRES 750	154	67.8	0.00141593	0.018910	0.001088	0.94	No
Orbit 218							
UVVIS 415	-	0.046	-	-	-	-	-
UVVIS 750	-	0.083	-	-	-	-	-
HIRES 415	159	51.8	0.00088803	0.016123	0.000570	0.95	No
HIRES 560	148	105.8	-	-	-		Few
HIRES 650	148	45.2	-	-	-		Few
HIRES 750	154	60.0	0.00138333	0.001110	0.001110	0.98	No
Orbit 220							
UVVIS 415	-	0.063	-	-	-	-	-
UVVIS 750	-	0.112	-	-	-	-	-
HIRES 415	156	60.4	0.00104305	0.01294000	0.00083207	0.98	No
HIRES 560	125	121.8	-	-	-		Yes
HIRES 650	145	50.8	-	-	-		Yes
HIRES 750	151	67.7	0.00165436	0.01749700	0.00139190	0.90	No
Orbit 224							
UVVIS 415	-	0.059	-	-	-	-	-
UVVIS 750	-	0.103	-	-	-	-	-
HIRES 415	156	56.3	0.00104796	0.012100	0.000836	0.96	No
HIRES 560	125	112.8	-	-	-		Yes
HIRES 650	145	46.4	-	-	-		Yes
HIRES 750	151	62.3	0.00165329	0.014489	0.001422	0.98	No

[a]MCP is the MicroChannel Plate (MCP) gain setting, Average is the mean value of the partially calibrated (background subtraction and nonuniformity correction) mosaic for HIRES and the fully calibrated IOF mosaic for UVVIS, Ratio is the average value of a ratio between matching HIRES and UVVIS mosaics, Constant (c) and Mult (m) represent the linear fit variables between HIRES and UVVIS (equation (4)). Gain and Offset Settings for all the HIRES images in this table were 4 and 5, respectively; all the images were acquired with an exposure time of 1.07 ms. Lat/Lon ranges Orbit 214, 52°S to 57°S 124.5°W to 125.5°W: Orbit 218, 55°S to 59°S, 136°W to138°W: Orbit 220, 49°S to 41°S, 140.8°W to 141.2°W: Orbit 224, 43°S to 46°S, 151.2°W to 151.6°W.

Table 3. Summary of Fits Between Orbit 214 HIRES and UVVIS Mosaics for 415-nm and 750-nm Wavelengths for Seven Areas (Each Area Represents 200 Lines and Overlaps by 100 Pixels From the Previous Area)[a]

	Constant (c)	Multiplier (m)	Ratio
Lha (415-nm), orbit 214, 7 areas			
Area 1	0.01590000	0.00061500	0.000868288
Area 2	0.01600000	0.00061900	0.000880527
Area 3	0.01120000	0.00069100	0.000880332
Area 4	0.01530000	0.00060900	0.000886316
Area 5	0.01570000	0.00061000	0.000889145
Area 6	0.01420000	0.00063100	0.000871199
Area 7	0.01250000	0.00065400	0.000889208
Average	0.01440000	0.00063271	0.000880716
Stand dev	0.00187972	0.00003009	0.000008363
Median	0.01530000	0.00061900	0.000880527
Values from whole mosaic	0.013219	0.000654	0.00088696
Lhd (750-nm), orbit 214, 7 areas			
Area 1	0.02320000	0.00103000	0.00134675
Area 2	0.02060000	0.00107000	0.00135772
Area 3	0.01360000	0.00116000	0.00135763
Area 4	0.01750000	0.00111000	0.00137675
Area 5	0.01720000	0.00112000	0.00138165
Area 6	0.01870000	0.00108000	0.00135405
Area 7	0.02040000	0.00105000	0.00138048
Average	0.01874286	0.00108857	0.00136500
Stand dev	0.00306695	0.00004451	0.00001423
Median	0.01870000	0.00108000	0.00135772
Values from whole mosaic	0.018910	0.001088	0.00141593

[a]Constant and Multiplier represent the variables in c and m, respectively, in equation (3). The column labeled ratio is the average value of all pixels in the ratio imaged formed by the UVVIS/HIRES mosaics, per area. Gain and Offset Settings for all the HIRES images in this table were 4 and 5, respectively; all the images were acquired with an exposure time of 1.07 ms. UVVIS = (m × HIRES) + c.

Table 4. Summary of Fits Between Orbit 220 HIRES and UVVIS Mosaics for 415-nm and 750-nm Wavelengths for 11 Areas (Each Area Represents 200 Lines and Overlaps by 100 Pixels From the Previous Area)[a]

	Constant (c)	Multiplier (m)	Ratio
Lha (415-nm), orbit 220, 11 areas			
Area 1	0.02310000	0.00069400	0.00102392
Area 2	0.02050000	0.00073000	0.00101626
Area 3	0.01550000	0.00080500	0.00103010
Area 4	0.01230000	0.00084900	0.00105015
Area 5	0.02190000	0.00068400	0.00106445
Area 6	0.02070000	0.00070300	0.00104782
Area 7	0.01420000	0.00081400	0.00103964
Area 8	0.00966000	0.00088600	0.00105389
Area 9	0.01640000	0.00075500	0.00107731
Area 10	0.01620000	0.00075500	0.00107035
Area 11	0.01530000	0.00076600	0.00105854
Average	0.01688727	0.00076745	0.00104840
Stand Dev	0.00420673	0.00006518	0.00001938
Median	0.01620000	0.00075600	0.00105015
Values from whole mosaic	0.01294000	0.00083207	0.00104305
Lhd (750-nm), orbit 220, 11 areas			
Area 1	0.03480000	0.00116000	0.00160478
Area 2	0.02360000	0.00130000	0.00159480
Area 3	0.01580000	0.00142000	0.00162357
Area 4	0.01200000	0.00148000	0.00164970
Area 5	0.02320000	0.00132000	0.00167415
Area 6	0.02600000	0.00127000	0.00165422
Area 7	0.01290000	0.00145000	0.00163666
Area 8	0.01220000	0.00147000	0.00166071
Area 9	0.01220000	0.00148000	0.00169072
Area 10	0.01310000	0.00146000	0.00167944
Area 11	0.01230000	0.00146000	0.00166861
Average	0.01800909	0.00138818	0.00164885
Stand Dev	0.00771537	0.00010824	0.00003089
Median	0.01310000	0.00145000	0.00165422
Values from whole mosaic	0.017497	0.001392	0.00165436

[a]Constant and Multiplier represent the variables in c and m, respectively, in equation (3). The column labeled ratio is the average value of all pixels in the ratio imaged formed by the UVVIS/HIRES mosaics. Gain and offset settings for all the HIRES images in this table were 4 and 5 respectively, all the images were acquired with an exposure time of 1.07 ms. UVVIS = (m × HIRES) + c.

**Table 5.** Absolute Coefficients Per Gain State for Clementine HIRES Camera Filter 415-nm (lha)[a]

Orbit	MCP Gain	Absolute Coefficient
224	156	0.00105 ± 0.000040
220	156	0.00105 ± 0.000046
218	159	0.00089 ± 0.000048
214	159	0.00089 ± 0.000046

[a]Coefficient is calculated from the average value of a ratio of the UVVIS mosaic over the HIRES mosaic per a given orbit; the standard deviation is shown as an indication of the precision of the value (see Table 3). Gain and offset settings for all the HIRES images in this table were 4 and 5, respectively; all the images were acquired with an exposure time of 1.07 ms.

Table 6. Absolute Coefficients Per Gain State for Clementine HIRES Camera Filter 750-nm (lhd)[a]

Orbit	MCP Gain	Absolute Coefficient
224	151	0.00166 ± 0.000042
220	151	0.00165 ± 0.000048
218	154	0.00138 ± 0.000041
214	154	0.00137 ± 0.000053
N. Pole	158	0.00097 ± 0.000350

[a]N. Pole refers to HIRES mosaic shown in Figure 22. Coefficient is calculated from the average value of a ratio of the UVVIS mosaic over the HIRES mosaic per a given orbit; the standard deviation is shown as an indication of the precision of the value (Table 4). Note that the standard deviation for the North Pole mosaic is ∼10X that of the other data. This is due to the fact the HIRES mosaic, composed of images from 63 orbits, was compared to UVVIS data taken from different orbits. Rapidly changing lighting conditions at the poles thus cause artifacts around topographic features (i.e., impact craters and basin massifs). Gain and offset settings for all the HIRES images in this table were 4 and 5, respectively; all the images were acquired with an exposure time of 1.07 ms.
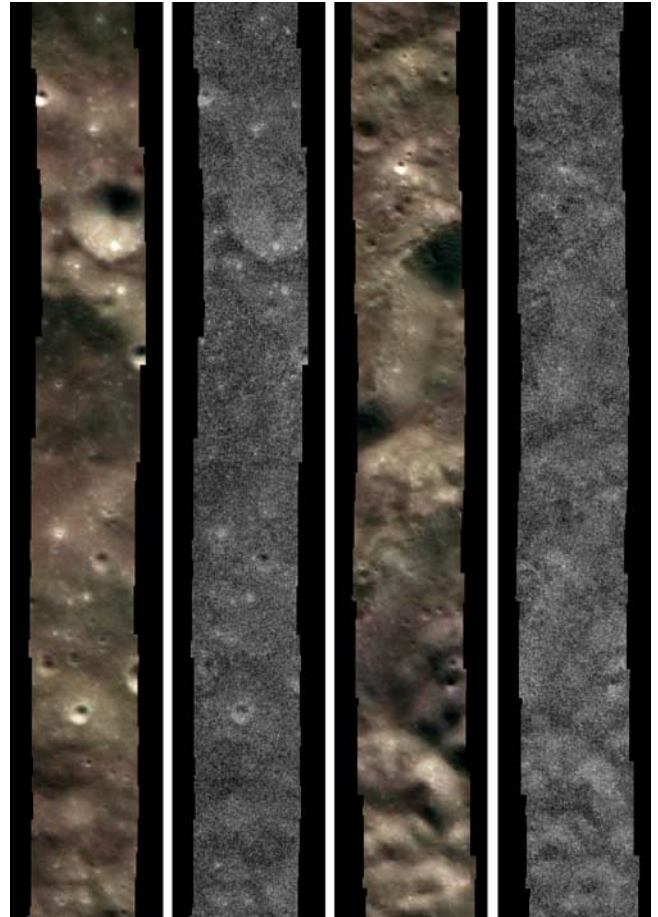
Figure 20. Color mosaic strip from orbit 218 shown in two parts (left latitude range 55°S to 57°S and right 57°S to 59°S, longitude range for both is 136°W to 138°W). Color is formed by portraying 415-nm as blue, 560-nm as green, and 750-nm as red. The relatively bland BW strip to the right of each color strip is a ratio the 415-nm/750-nm filters shown to demonstrate the goodness of relative calibration. Note that frame-to-frame boundaries, hot-spot, and chicken wire pattern are not visible.

Table A1. Shadow Values in HIRES Polar Images

	Image Name	Average	Standard Dev.	Samp:Line
	lhd5415r.050.cub	9	0.0	150:223
1	lhd5415r.050.cal	1.04606	0.0211681	150:223
	lhd5751r.060.cub	10	0.0	177:82
2	lhd5751r.060.cal	1.56232	0.0627842	177:82
	lhd5661r.064.cub	10	0.0	120:184
3	lhd5661r.064.cal	2.0689	0.0434782	120:184
	lhd5685r.072.cub	9.96444	0.185179	105:194
4	lhd5685r.072.cal	2.10386	0.198872	105:194
	lhd5682r.078.cub	8.93778	0.241559	77:265
5	lhd5682r.078.cal	1.09469	0.283027	77:265
	lhd5710r.086.cub	10	0.0	244:184
6	lhd5710r.086.cal	1.83166	0.0484815	244:184
	lhd5750r.092.cub	9	0.0	115:136
7	lhd5750r.092.cal	0.961463	0.0334248	115:136
	lhd5565r.098.cub	8.95111	0.215636	195:271
8	lhd5565r.098.cal	1.01081	0.230827	195:271
	lhd5614r.108.cub	9	0.0	233:202
9	lhd5614r.108.cal	0.925981	0.0268102	233:202
	lhd5632r.112.cub	9	0.0	149:208
10	lhd5632r.112.cal	1.03747	0.018489	149:208
	lhd5661r.116.cub	8.89333	0.208689	171:226
11	lhd5661r.116.cal	0.893851	0.310219	171:226
	lhd5687r.120.cub	9	0.0	214:148
12	lhd5687r.120.cal	0.789413	0.033165	214:148
	lhd5773r.133.cub	10	0.0	160:191
13	lhd5773r.133.cal	1.96167	0.0435003	160:191
	lhd5687r.136.cub	10	0.0	163:249
14	lhd5687r.136.cal	2.09406	0.055655	163:249
	lhd5900r.139.cub	10	0.0	96:33
15	lhd5900r.139.cal	1.93684	0.0414005	96:33
	lhd5701r.142.cub	9	0.0	18:222
16	lhd5701r.142.cal	1.20074	0.0140054	18:222
	lhd5661r.146.cub	10	0.0	303:118
17	lhd5661r.146.cal	1.85186	0.0406969	303:118
	lhd5698r.152.cub	9.87111	0.335077	97:157
18	lhd5698r.152.cal	1.92261	0.341261	97:157
	lhd5799r.156.cub	10	0.0	95:241
19	lhd5799r.156.cal	2.30421	0.0590591	95:241
	lhd5822r.159.cub	9	0.0	310:103
20	lhd5822r.159.cal	0.932561	0.0194926	310:103

UVVIS global multispectral map. To fully exploit the potential of these high-resolution color data for compositional analyses removal of topographic induced variations in incidence and emission angle are required [*Robinson and Jolliff*, 2002]. Such data might be available in the near future from stereo analysis of Clementine [*Cook et al.*, 2000] and Lunar Orbiter images [*Gaddis et al.*, 2001] or from future lunar missions.

Appendix A: Dark Correction Residuals

[25] Average values of deep shadows in HIRES images in the vicinity of the lunar North Pole (Table A1), using 15 × 15 box size were collected to determine the efficacy of the derived offset correction (see main text for details). Data reported from both raw and semicalibrated versions (DN, flat field corrected only). Most of these images contain mostly shadow. Illuminated regions typically have raw values of DN 40–100. For each pair of images the values represent raw (.cub) and partially calibrated data (.cal). Partially calibrated data have had background removed and nonuniformity correction applied.

References

Bussey, D. B. J., P. D. Spudis, and M. S. Robinson, Illumination conditions at the lunar south pole, *Geophys. Res. Letters*, 26, 1187–1190, 1999.

Charette, M. P., T. B. McCord, C. Pieters, and J. B. Adams, Application of remote spectral reflectance measurements to lunar geology classification and determination of titanium contents of lunar soils, *J. Geophys. Res.*, 79, 1605–1613, 1974.

Charette, M. P., L. A. Soderblom, J. B. Adams, M. J. Gaffey, and T. B. McCord, Age-color relationships in lunar highlands, *Proc. Lunar Sci. Conf. 7th*, 2579–2592, 1976.

Cook, A. C., T. R. Watters, M. S. Robinson, P. D. Spudis, and D. B. J. Bussey, Lunar polar topography derived from Clementine stereo images, *J. Geophys. Res.*, 105, 12,023–12,033, 2000.

Gaddis, L. R., T. Sucharski, T. Becker, and A. Gitlin, Cartographic processing of digital lunar orbiter data, *Lunar Planet. Sci. XXXII*, abstract 1892, 2001.

Lucey, P. G., G. J. Taylor, and E. Malaret, Abundance and distribution of Iron on the Moon, *Science*, 268, 1150–1153, 1995.

Lucey, P. G., D. T. Blewett, and B. Ray Hawke, Mapping the FeO and TiO$_2$ content of the lunar surface with multispectral imagery, *J. Geophys. Res.*, 103, 3679–3699, 1998.

Malaret, E., L. Perez, and H. Taylor, ACT's Final report Clementine's UVVIS camera in-flight calibration results, *ACT Int. Memo.*, Appl. Coherent Technol. Corp., Herndon, Va., 1999.

McEwen, A. S., and M. S. Robinson, Mapping of the Moon by Clementine, *Adv. Space Res.*, *19*, 1523–1533, 1997.

Minnaert, M., Photometry of the Moon, in *Planets and Satellites*, edited by G. Kuiper and B. M. Middlehurst, pp. 213–248, Univ. of Chicago Press, Chicago, Ill., 1960.

Nozette, S., and H. B. Garrett, Mission offers a new look at the Moon and a near-Earth asteroid, *Eos Trans. AGU*, *75*, 161, 1994.

Nozette, S., et al., The Clementine mission to the Moon: Scientific Overview, *Science*, *266*, 1835–1839, 1994.

Robinson, M. S., and B. L. Jolliff, Apollo 17 landing site: Topography, photometric corrections, and heterogeneity of the surrounding highland massifs, *J. Geophys. Res.*, *107*(E11), 5110, doi:10.1029/2001JE001614, 2002.

Shoemaker, E. M., M. S. Robinson, and E. M. Eliason, The south pole region of the Moon as seen by Clementine, *Science*, *266*, 1851–1854, 1994.

Sorensen, T. C., Global lunar mapping by the Clementine spacecraft, Paper AAS 95–127, *Adv. Astronaut. Sci.*, *89*, 457–476, 1995.

White, T., and B. Wilson, HiRes "Hysteresis" Measurements, 11/7/94, *Internal Memo*, Lawrence Livermore Natl. Lab., Livermore, Calif., 1994.

———————————

E. Malaret, Applied Coherent Technology Corporation, 112 Elden Street, Suite K, Herndon, VA 22070, USA. (malaret@actgate.com)

M. S. Robinson, Center for Planetary Sciences, Northwestern University, 1850 Campus Drive, Evanston, IL 60208, USA. (robinson@earth.northwestern.edu)

T. White, Lawrence Livermore National Laboratory, Livermore, CA 94550, USA. (wtw@llnl.gov)